Proceedings of the Sixth International Conference on Engineering Computational Technology

Edited by
M. Papadrakakis and B.H.V. Topping

Athens - Greece
2-5 September 2008

CIVIL-COMP PRESS

published 2008 by
Civil-Comp Press
Dun Eaglais, Kippen
Stirlingshire, FK8 3DY, UK

Civil-Comp Press is an imprint of Civil-Comp Ltd

ISBN 978-1-905088-24-9 (Book)
ISBN 978-1-905088-25-6 (CD-Rom)
ISBN 978-1-905088-26-3 (Combined Set)

British Library Cataloguing in Publication Data
A catalogue record for this book is available from the British Library

Cover Image: mesh created by R. Montenegro and G. Montero based on the "25 Years of Civil-Comp Conferences" logo.

Printed in Great Britain by Bell & Bain Ltd, Glasgow

Paper 143

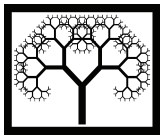

Proceedings of the Sixth International Conference
on Engineering Computational Technology,
M. Papadrakakis and B.H.V. Topping, (Editors),
Civil-Comp Press, Stirlingshire, Scotland

Modelling Nonlinear Electro-Mechanical Effects in Nano-Heterostructures Using Domain-Decomposition Methods

L.X. Wang[1], M. Willatzen[2] and R.V.N. Melnik[3]
[1] Faculty of Mechanical Engineering
Hangzhou Dainzi University, Xiasha, Hangzhou, P.R. China
[2] MCI, University of Southern Denmark, Denmark
[3] M[2]NeT Lab, Wilfrid Laurier University, Waterloo, Canada

Abstract

In this work, a continuum three-dimensional axi-symmetrical model for a nonlinear-coupled multiphysics system is constructed accounting for self-consistency in electromechanical fields. A cylindrical GaN/AIN wurtzite nano-heterostructure is considered so as to simplify the mathematical problem to a two-dimensional model. To cope with the inherent discontinuity of the physical parameters and lattice mismatch across the interface, the domain-decomposition strategy is combined together with the Chebyshev spectral methods for the numerical analysis of the nonlinear problem. We report numerical results in the current presentation. We provide details on continuous mechanical and electric displacements and quantify jumps of discontinuities in the electric fields and strain distributions occurring across the interface between the two material. The importance of using a nonlinear model (with electrostriction) is investigated by comparison with a linear model (without electrostriction). We also point out significant differences qualitatively in the self-consistent electric fields and strains found using a two-dimensional and a one-dimensional model analysis.

Keywords: Heterostructures, lattice mismatch, electrostriction, piezoelectric, spectral methods.

1 Introduction

GaN/AIN heterostructures have attracted a great deal of efforts from physicists and mathematicians due to their application potential in optoelectronic devices [3]. Recently, the problem has been investigated self-consistently in lattice mismatch, spontaneous polarization, piezoelectric effects, and strains employing a linear (static and dynamic approaches) and nonlinear (static approach with electrostriction) electrome-

chanical model framework [4, 5] all based on a one-dimensional model. Two-dimensional self-consistent effects accounting for nonlinear electrostrictive effects have, to our knowledge, not yet been addressed in spite of the belief that a combination of dimensional effects and electrostriction could lead to interesting new physics. This lack of attention reflects to a large extent the sparse information available about electrostriction-tensor components in the nitrides.

In the current work, a continuum three-dimensional axisymmetrical model for the nonlinear-coupled multi-physics system is constructed accounting for complete self-consistency in electromechanical fields. A cylindrical wurtzite GaN/AIN nano-heterostructure is considered so as to simplify the mathematical problem to a two-dimensional model. Note that albeit the wurtzite symmetry is not axisymmetric, Navier's equations with the boundary conditions imposed do reflect axisymmetry [6].

2 Mathematical Modeling

Consider the heterostructure as sketched in Figure 1 consisting of a GaN thin film grown on an AIN substrate. The thickness and radius of the thin film is 10 and 20 nanometer, respectively. The substrate is modelled as a 100 nanometer thick layer with the same radius as the film layer.

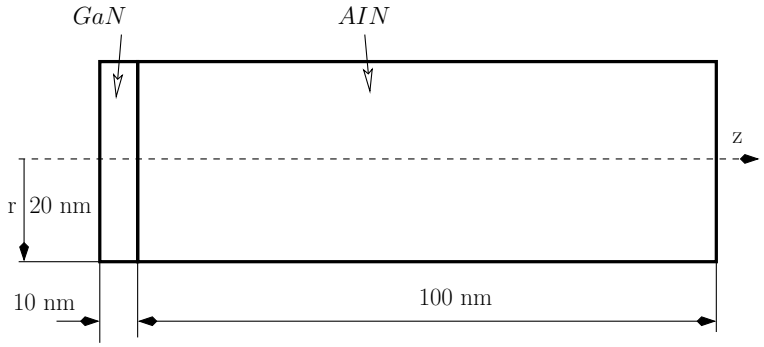

Figure 1: Two-dimensional analog of a cylindrical nano-heterostructure.

It is assumed that the problem is axisymmetric allowing for a two-dimensional mathematical analysis as shown in the figure. In order to take into account lattice mismatch effects between the thin film and substrate layers, the following representation of the strain tensor S is introduced:

$$\begin{aligned} S_{rr} &= \frac{\partial u_r}{\partial r} - \frac{a(r)-a^1}{a^1}, \;\; S_{\phi\phi} = \frac{u_r}{r} - \frac{a(r)-a^1}{a^1}, \\ S_{zz} &= \frac{\partial u_z}{\partial z} - \frac{c(r)-c^1}{c^1}, \;\; S_{rz} = \frac{1}{2}\left(\frac{\partial u_r}{\partial z} + \frac{\partial u_z}{\partial r}\right), \\ S_{r\phi} &= 0, \;\; S_{\phi z} = 0, \end{aligned} \tag{1}$$

where $u_r,\ u_z$ are displacements along the $r,\ z$ directions, respectively. Similarly, $a(r), a^1, c(r), c^1$ are the in-plane (thin film) nanostructure, in-plane substrate, perpendicular (thin film) nanostructure, and perpendicular substrate lattice constants, respectively.

The constitutive laws for the materials accounting for the piezoelectric and electrostriction effects are as follows:

$$\begin{aligned}
T_{rr} &= c_{11}^E S_{rr} + c_{12}^E S_{\phi\phi} + c_{13}^E S_{zz} - e_{31} E_z, \\
T_{\phi\phi} &= c_{12}^E S_{rr} + c_{11}^E S_{\phi\phi} + c_{13}^E S_{zz} - e_{31} E_z, \\
T_{zz} &= c_{13}^E S_{rr} + c_{13}^E S_{\phi\phi} + c_{33}^E S_{zz} - e_{33} E_z + M_z^T E_z^2, \\
T_{rz} &= c_{44}^E S_{rz} - e_{15} E_r,\ T_{\phi z} = T_{r\phi} = 0, \\
D_r &= e_{15} S_{rz} - \varepsilon_{11} E_r,\ \ D_\phi = 0, \\
D_z &= e_{31} S_{rr} + e_{31} S_{\phi\phi} + e_{33} S_{zz} + \varepsilon_{33} E_z + 2 M_T^E T_{zz} E_z,
\end{aligned} \tag{2}$$

where e, c, ε are material coefficients, M_z^T, M_T^E are electrostriction related coefficients. E_z and E_r are two components of the electric field in the considered domain and defined as $-\nabla P$ with P is the electric potential.

Experimental information about electrostriction coefficient is scarce and to the best of our knowledge only the coefficient connecting the electric field along the z direction with the strain component S_{zz} has been reported [7]. Hence, we consider in the following only this single component of electrostriction. It is important to note that the current model can be easily extended to include the other two electrostriction coefficients possible by symmetry.

Based on the constitutive relationships (1) and (2), the governing equations for the system can be easily formulated by using the conservation laws, and read in cylindrical coordinates as follows:

$$\begin{aligned}
\frac{\partial T_{rz}}{\partial r} &+ \frac{\partial T_{zz}}{\partial z} + \frac{T_{rz}}{r} = 0, \\
\frac{\partial T_{rr}}{\partial r} &+ \frac{\partial T_{rz}}{\partial z} + \frac{T_{rr} - T_{\phi\phi}}{r} = 0, \\
\frac{\partial D_r}{\partial r} &+ \frac{\partial D_z}{\partial z} + \frac{D_r}{r} = 0,
\end{aligned} \tag{3}$$

where T and D are stresses and electric displacements, respectively, and r, z are the radial and axial coordinates, respectively.

The boundary conditions for the current problem are the following (length unit is nanometer):

$$\begin{aligned}
P(z,r) &= 0,\ T_{rz}(z,r) = 0,\ T_{zz}(z,r) = 0,\ \text{for z=0}, \\
P(z,r) &= 0,\ T_{rz}(z,r) = 0,\ u_z(z,r) = 0,\ \text{for z=110}, \\
D_r(z,r) &= 0,\ T_{rz}(z,r) = 0,\ T_{rr}(z,r) = 0,\ \text{for r=20},
\end{aligned} \tag{4}$$

The well-posedness of this model in the linear case was established in [9].

3 Chebyshev Collocation Method

In order to analyze the system given by Equations (3) and (4), one has to apply numerical methods for the purpose. The Chebyshev pseudo-spectral method is employed here for the numerical simulation, because it has a higher accuracy with a relatively smaller number of discretization nodes compared to other methods, such as finite element or finite difference methods [1, 8]. As a result, this methodology has recently been applied successfully in the context of other coupled nonlinear multiphysics problems [10, 11, 12].

We start the discussion with the numerical approximation of the one-dimensional analogue of the above model in a single domain first, in which there is no discontinuity of the material properties and no lattice mismatch. Therefore all functions are smooth in the considered domain. In order to approximate a smooth function in the one-dimensional case on discrete nodes using the Chebyshev pseudo-spectral method, a set of Chebyshev points $\{z_i\}$ are chosen as follows:

$$z_i = (z_b - z_a)\left(1 + \cos\left(\frac{\pi i}{N}\right)\right)/2 + z_a, \quad i = 0, 1, \ldots, N, \tag{5}$$

where $[z_a, z_b]$ is the computational domain, and $N + 1$ is the number of nodes chosen for the approximation. Using these nodes, the displacements, stress, strain, electric field and displacement distributions in the considered domain can be expressed in terms of the following linear approximation:

$$f(z) = \sum_{i=0}^{N} f_i \phi_i(z), \tag{6}$$

where $f(z)$ can be any of the variables considered in the current problem and f_i is the function value at z_i. $\phi_i(z)$ is the i^{th} interpolating polynomial associated with z_i which has the following cardinality property:

$$\phi_i(z_j) = \begin{cases} 1, & i = j, \\ 0, & i \neq j. \end{cases} \tag{7}$$

It is easy to see that the well-known Lagrange interpolant satisfies the interpolation requirements. Having obtained $f(z)$ approximately, the derivative $\partial f(z)/\partial z$ can be easily obtained by taking the derivative of the basis functions $\phi_i(z)$ with respect to z:

$$\frac{\partial f}{\partial z} = \sum_{i=0}^{N} f_i \frac{\partial \phi_i(z)}{\partial z}. \tag{8}$$

Following the same idea as given in Ref [8], Equation (8) can be written in a matrix form as:

$$\mathbf{F_d} = \mathbf{DF}, \tag{9}$$

and the differentiation matrix $\mathbf{D}$ becomes:

$$\mathbf{D_{ij}} = \begin{cases} \dfrac{2N^2+1}{6} & i = j = 0, \\ -\dfrac{2N^2+1}{6} & i = j = N, \\ -\dfrac{z_j}{2(1-z_j^2)} & i = j = 1, 2, \ldots, N-1, \\ \dfrac{c_i}{c_j}\dfrac{(-1)^{i+j}}{(z_i - z_j)} & i \neq j, \quad i, j = 1, 2, \ldots, N-1, \end{cases} \tag{10}$$

where

$$c_i = \begin{cases} 2, & i = 0, N, \\ 1, & \text{otherwise.} \end{cases} \tag{11}$$

Obviously, $\mathbf{D_{ij}}$ is an $(N+1)\times(N+1)$ matrix. Here $\mathbf{F_d}$ and $\mathbf{F}$ are vectors collecting all values of the derivative $\partial f/\partial z$ and the function f at z_i, respectively.

For the present discussion, one needs to connect the potential given on the boundary to the electric field in the heterostructure, therefore an integral operator acting on the electrical field is necessary. This fact requires a quadrature rule using the same set of points as chosen for the derivative approximation. For the currently chosen discretization nodes, the quadrature can be done by using the Chebyshev-Lobatto rule which is exact for any polynomial with an order less than $2N + 1$ [1, 8] . The quadrature rule can be written as:

$$\int_a^b f(x)dx = \sum_{i=0}^{N} w_i f(z_i), \tag{12}$$

where weight coefficients w_i for the quadrature can be easily obtained using the idea given in Ref.[1, 2].

For the extension of the Chebyshev spectral approximation from the one-dimensional case to higher dimensions, an easy choice is to apply Equation (5) for choosing the Chebyshev points in both z and r directions in the current problem, such that the two-dimensional function approximation is formulated by using tensor products as follows:

$$f(z, r) = \sum_{i=0}^{N}\sum_{j=0}^{M} f_{i,j}\phi_i(z)\phi_j(r), \tag{13}$$

where M is the number of nodes chosen for the approximation in the r direction and $\phi_j(r)$ is the j^{th} interpolant in the r direction. In two dimensional cases, the disrcretization nodes are numbered by using the "lexicographic" ordering, such that the differentiation matrices in the two-dimensional case are constructed by using the Kronecker products as follows:

$$\mathbf{D_z} = \mathbf{I} \otimes \mathbf{D}, \quad \mathbf{D_r} = \mathbf{D} \otimes \mathbf{I}, \tag{14}$$

where $\mathbf{I}$ is the identity matrix, $\mathbf{D_z}$ ($\mathbf{D_r}$) is the differentiation matrix corresponding to $\partial f/\partial z$ ($\partial f/\partial r$). The construction of differentiation matrices for higher-order derivatives are implemented in a similar way.

4 Domain decomposition and implementation

In the present case with GaN/AIN heterostructures, a discontinuity in material properties occurs at the interface of the heterostructure. Furthermore, a lattice mismatch-induced strain component discontinuity exists at the interface. Therefore, it is natural to introduce a multi-domain method to circumvent the numerical difficulties in the analysis of the heterostructure problem. Hence, the whole heterostructure $\mathcal{D}$ as sketched in Figure. 1 is decomposed into two subdomains corresponding to the two different materials:

$$\mathcal{D} = \bigcup_{d=1}^{d=2} \mathcal{D}^d, \tag{15}$$

The first subdomain ($d = 1$) corresponds to the domain occupied by the thin film whilst the second one ($d = 2$) is associated with the substrate. Thus, in each subdomain, all the variables and material properties and their derivatives are smooth, and these functions can be reasonably well approximated by linear combinations of the basis functions in the subdomain:

$$f^d(z,r) = \sum_{i=0}^{N^d} \sum_{j=0}^{M^d} f^d_{i,j} \phi^d_i(z) \phi^d_j(r), \tag{16}$$

where $f^d(z,r)$ is the function approximated in the d^{th} subdomain, $N^d + 1$ is the number of nodes for the approximation in the subdomain in the z direction, $f^d_{i,j}$ is the function value in the (i,j) node in the d^{th} subdomain, $\phi^d_i(z)$ and $\phi^d_j(r)$ are basis functions in the d^{th} subdomain for the z and r directions, respectively. The superscript indicates the subdomain.

The following interface conditions apply:

$$\begin{array}{rcll} u^1_z(\bar{z},r) & = & u^2_z(\bar{z},r), & u^1_r(\bar{z},r) = u^2_r(\bar{z},r), \\ T^1_{zz}(\bar{z},r) & = & T^2_{zz}(\bar{z},r), & T^1_{rz}(\bar{z},r) = T^2_{rz}(\bar{z},r), \\ P^1(\bar{z},r) & = & P^2(\bar{z},r), & D^1_z(\bar{z},r) = D^2_z(\bar{z},r), \end{array} \tag{17}$$

where $(\bar{z},r)$ is the location of the interface between the two subdomains $\mathcal{D}^1$ and $\mathcal{D}^2$. The above coupling conditions correspond to continuity in stress, mechanical and electric displacements, as well as electric potential, as required by the physics of the problem.

For the current problem, the whole computational domain is given as $\mathcal{D} = [0, 110] \times [0, 20]$ in nm^2 which is half of the domain sketched in Figure 1 due to the symmetry

conditions. The computational domain is then decomposed into two subdomains as $\mathcal{D} = [0, 10] \times [0, 20] \bigcup [10, 110] \times [0, 20]$ where $[0, 10] \times [0, 20]$ is the subdomain associated with the thin film discretized using $N^1 + 1$ nodes in the z direction and $M^1 + 1$ nodes in the r direction. Similarly, the subdomain $[10, 110] \times [0, 20]$ is associated with the substrate discretized using $(N^2 + 1) \times (M^2 + 1)$ nodes. By employing approximations to the derivatives and integral operators as mentioned above, the system given by Equation (3) can be recast into the following algebraic system:

$$\begin{aligned} \mathcal{G}_{U_z}(\mathbf{U_z}, \mathbf{U_r}, \mathbf{P}) &= 0, \\ \mathcal{G}_{U_r}(\mathbf{U_z}, \mathbf{U_r}, \mathbf{P}) &= 0, \\ \mathcal{G}_{P}(\mathbf{U_z}, \mathbf{U_r}, \mathbf{P}) &= 0, \end{aligned} \tag{18}$$

where $\mathbf{U_z}$ is a vector with a length of $(N^1 + 1) \times (M^1 + 1) + (N^2 + 1) \times (M^2 + 1)$ collecting all the displacement values u_z on the discretization nodes we are seeking for. Similarly, $\mathbf{U_r}$ is a vector corresponding to u_r, and $\mathbf{P}$ is a vector corresponding to the electric potential P. $\mathcal{G}_{U_z}$ is a collection of all the algebraic functions defined by the spatial discretization of the first equation given in Equation (3), $\mathcal{G}_{U_r}$ is the collection of algebraic equations associated with the second equation, while $\mathcal{G}_P$ is associated with the third one.

Boundary conditions and coupling conditions at the interface can be implemented by making a suitable modification to Equation (18). Thus, boundary conditions and coupling conditions are discretized together with the set of governing equations. Equation (18) must be replaced by the discretized form of Equation (4) and (18). The modified system is a nonlinear algebraic equation system with the same size as Equation (18) which is solved by using the Newton-Raphson iterative method.

Parameters	WZ GaN	WZ AIN		Parameters	WZ GaN	WZ AIN
a(nm)	3.189	3.112		c(nm)	5.185	4.982
C_{11} (GPa)	390	396		C_{12}(GPa)	145	137
C_{13} (GPa)	106	108		C_{33}(GPa)	398	373
C_{44}(GPa)	105	116		$e_{15}(C/m^2)$	-0.49	-0.60
$e_{31}(C/m^2)$	-0.49	-0.60		$e_{33}(C/m^2)$	0.73	1.46

Table 1: Material parameters used in the computations.

5 Numerical Results

In this section, numerical results of the current problem are presented. The parameter values used in the computation are given in Table 1 from Ref. [13]. We emphasize that there is much uncertainty related to the electrostriction coefficient of GaN. In Ref. [7], a giant value: $M_T^E = 1.2 \times 10^{-18} \frac{C}{m \cdot vP_a}$ [7] was reported being two-three orders of magnitude larger than those reported for other similar semiconductors. We

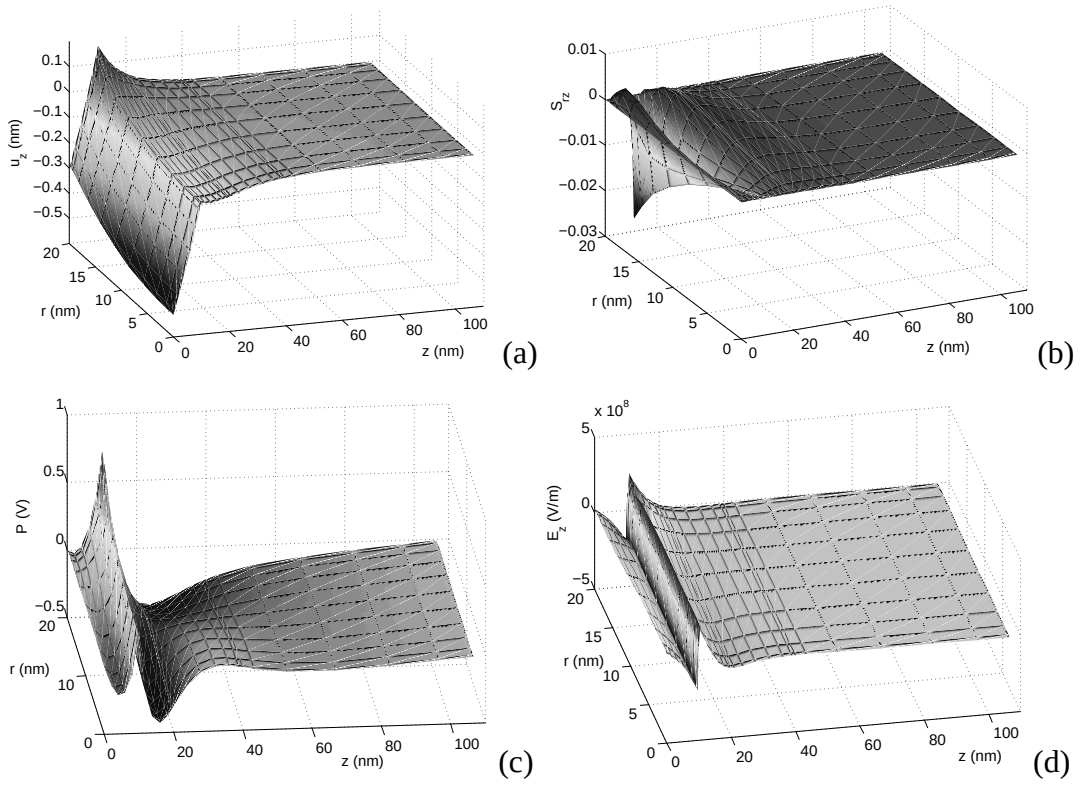

Figure 2: Numerical results accounting for electrostriction in the GaN/AIN nano-heterostructure. (a) Displacement in the z direction; (b) Strain component S_{rz}; (c) Potential in the structure; (d) Electric fields in the z direction.

have recently carried out ab-initio calculations indicating that the GaN electrostriction value is approximately three orders of magnitude smaller than that given by Ref. [7] which is in good agreement with those known for other similar wurtzite and zincblende crystals. Hence, we use in this work the values $M_T^E = 1.2 \times 10^{-21} \frac{C}{m \cdot v P_a}$ and $M_z^T = 3.5 \times 10^{-7} \frac{P_a m^2}{V^2}$. The number of discretization nodes for the thin film is $N^1 = 15, M^1 = 23$ while those for the substrate are $N^2 = 45, M^2 = 23$. To illustrate the influence of electrostriction effects together with the lattice mismatch, the displacements in the z direction, the strain S_{rz}, the electric potentials P, and the electric field component in the z direction E_z are analyzed numerically and presented here.

As sketched in Figure 2, the continuity of the displacement in the z direction across the interface is successfully modelled while the strain S_{rz} shows an abrupt jump due to the heterogeneity. The potential is continuous across the interface but the electric field is not. Considering that electrostriction effects are proportional to the square of the electric field in addition to the jump in the electric field along the z direction (across the interface) shows that electrostrictive contributions are most important near the interface. This coupled with lattice mismatch may cause numerical difficulties

especially for larger electrostriction coefficient values. This adds to the importance of obtaining further data for electrostriction coefficients in these important material compounds. We emphasize also that if electrostriction coefficients of GaN indeed are near the experimentally reported value [7], huge effects of electrostriction on self-consistent electromechanical fields will result.

To assess the importance of electrostriction, the system is also analyzed by setting $M_T^E = M_z^T = 0$, i.e., in the absence of electrostriction. The system variables, u_z, S_{rz}, P_z, and E_z are presented in Figure 3 by plotting the difference between results obtained in cases with and without electrostriction. By comparing the plots in Figure 3 with their counterparts in Figure 2, it is evident that electrostriction gives important contributions especially near the interface. As stipulated above, electrostriction adds to the strength of the abrupt jumps in the electric field across the interface induced by lattice mismatch.

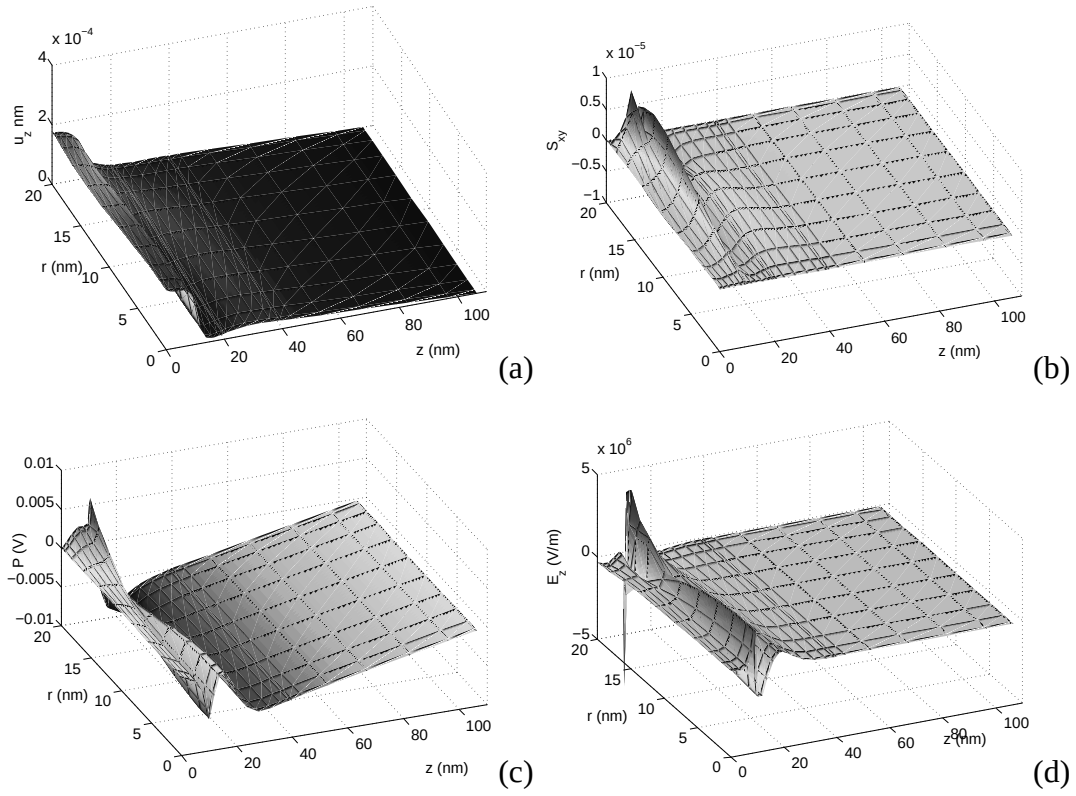

Figure 3: The difference of physical fields in the GaN/AIN nano-heterostructure between the case with and without electrostriction. (a) Displacement in the z direction; (b) Strain component S_{rz}; (c) Potential in the structure; (d) Electric fields in the z direction.

We next comment on the differences between a one-dimensional approach and the two-dimensional one used here. By looking at the plots presented here in Figure 2 and 3, it is evident that the modelled variables are far from being uniform along

the r direction, a characteristic that a one-dimensional model in z cannot capture thus demonstrating the importance of using a full geometrical analysis of realistic GaN/AlN nanostructures.

6 Conclusion

In this paper, a continuum two-dimensional model for the nonlinear-coupled multi-physics in a cylindrical GaN/AIN nano-heterostructure system has been constructed accounting for self-consistency in electromechanical fields. The lattice mismatch, piezoelectric, and electrostriction effects have been accounted for. The Chebyshev spectral method has been applied for the numerical analysis and a domain-decomposition strategy has been employed to deal with the discontinuity. Numerical results have been presented for key physical and mechanical field distributions in a typical layered heterostucture and the effects of electrostriction have been analyzed. It is shown that electrostriction are most important near the interface and that a two-dimensional model gives qualitative differences as compared to a one-dimensional model for electromechanical fields in wurtzite GaN/AlN three-dimensional nanostructures.

References

[1] A. Quarteroni, R. Sacco, and F. Saleri, *Numerical Mathematics*, Springer-Verlag, Berlin, Heidelberg, New York, 2000.

[2] G.Gautschi, Orthogonal polynomials and quadrature,*Electronic Transaction on Numerical Algorithm*, Vol 9,65-76, 1999.

[3] J. Piprek, *Nitride Semiconductor Devices - Principles and Simulation*, Wiley, New York (2007).

[4] M. Willatzen, B. Lassen, L.C. Lew Yan Voon, and R.V.N Melnik, Dynamic coupling of piezoelectric effects, spontaneous polarization, and strain in lattice-mismatched semiconductor quantum-well heterostructures, *J. Appl. Phys.*, 100, 024302 (2006).

[5] M. Willatzen, L. Wang, and L.C. Lew Yan Voon, Electrostriction in GaN/AlN heterostructures, to appear in *Superlattices and Microstructures* (2007).

[6] L.C. Lew Yan Voon, C. Galeriu, B. Lassen, M. Willatzen, and R.V.N. Melnik, Electronic structure of wurtzite quantum dots with cylindrical symmetry, *Applied Physics Letters*, 87, 041906 1-3, (2005). Also published in *the Virtual Journal of Nanoscale Science & Technology*, August 1, 2005.

[7] I.L. Guy, S. Muensit, and E.M. Goldys, Electrostriction in GaN, *Appl. Phys. Lett.*, 75, 3641-3643 (1999).

[8] L. N. Trefethen,*Spectral method in Matlab*, SIAM, Philadelphia, 2000.

[9] R.V.N. Melnik, Generalised solutions, discrete models and energy estimates for a 2D problem of coupled field theory, *Applied Mathematics and Computation*, 107 (1), 27-55, (2000).

[10] L.X. Wang, R.V.N. Melnik, Mechanically induced phase combination in shape memory alloys by Chebyshev collocation methods, *Materials Science and Engineering A -Structural Materials Properties Microstructure and Processing*, 438, SI, 427-430, (2006).
[11] L.X. Wang, R.V.N. Melnik, Numerical model for vibration damping resulting from the first-order phase transformations, *Applied Mathematical Modelling*, 31 (9), 2008-2018, (2007)
[12] L.X. Wang, R.V.N. Melnik, Thermo-mechanical wave propagations in shape memory alloy rod with phase transformations, *Mechanics of Advanced Materials and Structures*, 14 (8), 665-676, (2007).
[13] V. Fonoberov and A. Balandin, Optical properties of wurtzite and zinc-blende GaN/AIN quantum dots, *J. Vac. Sci. Technol. B*, 22(4), 2190 - 2194, (2004)

Proceedings of the Sixth International Conference on Engineering Computational Technology

Edited by M. Papadrakakis and B.H.V. Topping

This book contains the summaries of the contributed papers presented at the Sixth International Conference on Engineering Computational Technology, held in Athens, Greece, 2-5 September 2008.

The full length papers are available in electronic format on the accompanying CD-ROM. The topics covered include:

- High Performance Computing
- Fluid-Structure Interaction
- Quantification of Uncertainty
- Interfaces
- Decision Making
- Multiscale Simulation
- Mesh Generation and Adaption
- Information Modeling
- Computational Linear Algebra
- Genectic Algorithms
- Parallel Computations
- Distributed Computing
- Computational Fluid Dynamics
- Optimization
- Meshless Methods
- Discrete Finite Element Methods
- Finite Element Solver Technology
- Boundary Element Methods
- Nano-Mechanics
- Particle Thermodynamics
- Computer Aided Engineering
- Computer Vision
- Biomedical Engineering
- Biomechanics
- Rock Mechanics
- Soil-Structure Interaction
- Geotechnical Engineering
- Environmental Engineering

A keyword and author index is provided both in this book and on the CD-ROM.

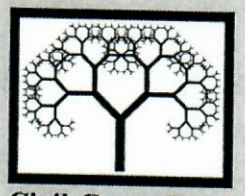

Civil-Comp Press

ISBN	978-1-905088-24-9	Book
ISBN	978-1-905088-25-6	CD-ROM
ISBN	978-1-905088-26-3	Combined Set


Proceedings of
The Sixth International Conference on
Engineering Computational Technology
CIVIL-COMP CONFERENCES
25
1983-2008
Civil-Comp Press
ISBN 978-1-905088-24-9 Book
ISBN 978-1-905088-25-6 CD-ROM
ISBN 978-1-905088-26-3 Set
COMPACT
disc
DATA STORAGE
© Copyright 2008
Civil-Comp Ltd.
All Rights Reserved
Edited by M. Papadrakakis and B.H.V. Topping
Athens - Greece
2-5 September 2008